

Zadoff-Chu sequence design for random access initial uplink synchronization

Md Mashud Hyder and Kaushik Mahata

Abstract—The autocorrelation of a Zadoff-Chu (ZC) sequence with a non-zero cyclically shifted version of itself is zero. Due to the interesting property, ZC sequences are widely used in the LTE air interface in the primary synchronization signal (PSS), random access preamble (PRACH), uplink control channel (PUCCH) etc. However, this interesting property of ZC sequence is not useful in the random access initial uplink synchronization problem due to some specific structures of the underlying problem. In particular, the state of the art uplink synchronization algorithms do not perform equally for all ZC sequences. In this work, we show a systematic procedure to choose the ZC sequences that yield the optimum performance of the uplink synchronization algorithms. At first, we show that the uplink synchronization is a sparse signal recovery problem on an overcomplete basis. Next, we use the theory of sparse recovery algorithms and identify a factor that controls performance of the algorithms. We then suggest a ZC sequence design procedure to optimally choose this factor. The simulation results show that the performance of most of the state of the art uplink synchronization algorithms improve significantly when the ZC sequences are chosen by using the proposed technique.

Index Terms—Random Access, initial synchronization, Zadoff-Chu sequence, sparse representation, OFDMA.

I. INTRODUCTION

A. Background

Many wireless communication systems adopt orthogonal frequency-division multiple access (OFDMA) technology for data transmission such as LTE [1], WiMAX [2] etc. To maintain orthogonality among the subcarriers in the uplink of OFDMA system, the uplink signals arriving at the eNodeB from different user equipments (UEs) should be aligned with the local time and frequency references. For this purpose, all UEs who want to set up connection to the eNodeB must go through an initial uplink synchronization (IUS) procedure. The IUS allows the eNodeB to detect these users, and estimate their channel parameters. These estimates are then used to time-synchronize UEs' transmissions and adjust their transmission power levels so that all uplink signals arrive at the eNodeB synchronously and at approximately the same power level [3]. The initial uplink synchronization is a contention based random access (RA) process. The process starts with the allocation of a pre-defined set of subcarriers called Physical Random Access Channel (PRACH) in some pre-specified time slots known as a "random access opportunity" [1]. The downlink synchronized UEs willing to commence communication, referred to as the synchronizing random access terminals (RTs), use this opportunity by modulating randomly

selected codes (also called RA preambles) from a pre-specified RA code matrix onto the PRACH. As the RTs are located in different positions within the radio coverage area, their signals arrive at the eNodeB with different time delays. At the receiving side, the eNodeB needs to detect the transmitted RA codes, and extract the timing and channel power information for each detected code [3]–[6].

The success of LTE in 4G cellular networks has made it popular. It is also envisaged that many of its key ingredients will also dominate the 5G systems. In this work, we consider the uplink data transmission protocol of an LTE-like system [6]. Zadoff-Chu sequences [7], [8] are used as random multiple access codes in the LTE system due to their perfect autocorrelation properties i.e., the autocorrelation of a ZC sequence with a non-zero cyclically shifted version of itself is zero. However, the eNodeB cannot fully exploit the perfect autocorrelation property of ZC sequences in different types of synchronization problems due to some factors. Hence, designing appropriate ZC sequences for different types of synchronization problems have received lots of research interests. A training-aided ZC sequence design procedure has been proposed in [9] for the frequency synchronization problem. The frequency synchronization deals with the estimation and compensation of carrier frequency offset (CFO) between the transmitter and a receiver. The CFO arises mainly due to the Doppler shift in downlink synchronization [3], [9]. The effect of carrier frequency offset on the autocorrelation property of the ZC sequences has been addressed in [10], [11]. A closed-form expression of the autocorrelation between two cyclically shifted ZC sequences in presence of frequency offset has been developed in [11]. Consequently, an empirical method has been proposed to design two different sets of ZC sequences: one for high frequency offset scenario and other for low frequency offset scenario, which can be used for the frequency offset estimation of UEs. The ZC sequence design for the timing synchronization problem has been addressed in [9], [12], [13]. The timing synchronization deals with the estimation of timing offset which arises due to the random propagation delay between eNodeB and user [9]. The method developed in [12] transmits partial Zadoff-Chu sequences on disjoint sets of equally spaced subcarriers for timing offset estimation. The signature sequences design procedure proposed in [13] considers the time and frequency synchronization in presence of carrier frequency offset between the eNodeB and single UE. To the best of our knowledge, the ZC sequence design for the IUS problem has not been addressed before. The IUS problem is different from the frequency and timing synchronization problems. In the IUS, the eNodeB has to detect multiple

Department of Electrical Engineering, The University of Newcastle, Australia.

RTs as well as extract their channel power and timing offset information. The effects of multiple-access interference (MAI) and unknown multipath channel impulse responses of RTs make the ZC sequence design problem challenging. In this work, we consider the ZC sequence design problem for the IUS purpose.

B. Some motivating examples

In this section, we observe that the performance of state of the art initial uplink synchronization (IUS) algorithms [3]–[6] can vary significantly depending on the RA code matrix. Moreover, the IUS algorithms may not yield the optimum performance with the RA code matrix generated by using the conventional procedure. To explain the matter, we first describe the procedure of RA code generation [1], [14].

To give example we consider the LTE system proposed in [6] where $N = 6144$. Total $M = 839$ number of adjacent subcarriers are allocated for the PRACH. The RA codes for the IUS are generated by cyclically shifting the Zadoff-Chu (ZC) sequence [7], [8]. The elements of the u -th root ZC sequence are given by

$$Z^u(k) = e^{-i\pi uk(k+1)/M}, \quad 0 \leq k < M \quad (1)$$

where u is a positive integer with $u < M$. Different RA codes are obtained by cyclically shifting the u -th root ZC sequence. Let $c_\ell^{(u)}$ be the ℓ -th RA code. Then the $(k+1)$ -th element of $c_{\ell+1}^{(u)}$ is given by

$$c_{k+1, \ell+1}^{(u)} = Z^u \{(k + \ell n_{cs}) \bmod M\}, \quad 0 \leq k < M. \quad (2)$$

Here $(\ell \bmod M) := \ell - M \cdot \lceil \ell/M \rceil$, with $\lceil r \rceil$ denoting the largest integer less than or equal to r . In addition, n_{cs} is an integer valued system parameter which is related to the wireless cell radius [10, eq. (17.10)]:

$$n_{cs} \geq \left\lceil \left(\frac{20}{3} \gamma - \tau_d \right) \frac{M}{T_{SEQ}} \right\rceil + n_g, \quad (3)$$

where $\lceil z \rceil$ is the smallest integer not less than z , γ is the cell radius (km), τ_d is the maximum delay spread (μ s), T_{SEQ} is the preamble sequence duration (μ s), and n_g is the number of additional guard samples. For a wireless cell radius of 1.3 km, typically $T_{SEQ} = 800\mu$ s, and $\tau_d < 1\mu$ s, which yields $n_{cs} \geq 11$. The maximum number of RA codes that can be generated from a single ZC root depends on the value of n_{cs} . For example, setting $n_{cs} = 11$, we can generate maximum $\lceil M/n_{cs} \rceil = 76$ RA codes from the ZC root u . If we need more than 76 RA codes then we have to utilize multiple roots. The procedure has been described explicitly in Section-IV-B.

Now, consider a RA uplink synchronization scenario where K number of RTs are simultaneously contending on the same PRACH channel. The channel impulse response of the RTs have a maximum order 35 and total $G = 50$ codes are available in the RA code matrix¹:

$$\mathbf{C} = [c_1^{(u)} \ c_2^{(u)} \ \cdots \ c_G^{(u)}].$$

¹In practice, there are 64 RA codes available in each cell. However, some codes are reserved for contention free RACH [14]. We assume that there are 14 reserve codes.

TABLE I
IUS USER DETECTION PROBABILITIES BY SOME ALGORITHMS FOR DIFFERENT VALUES OF u AND n_{cs} . SNR=10 dB, TOTAL IUS USERS $K = 3$ AND P_s DENOTES THE PROBABILITY OF SUCCESSFULLY DETECTING THE USERS.

Algorithm	P_s with $u = 1$					
	$n_{cs} = 11$	13	14	15	17	19
SMUD [4]	0.35	0.34	0.41	0.92	0.92	0.93
SRMD [5]	0.75	0.77	0.79	0.92	0.94	0.94
	P_s with $u = 2$			P_s with $u = 3$		
	$n_{cs} = 11$	13	17	11	13	17
SMUD [4]	0.19	0.3	0.4	0.77	0.34	0.29
SRMD [5]	0.41	0.59	0.73	0.84	0.72	0.39

We can generate different RA code matrices by using different values of u and $n_{cs} \geq 11$. Table-I shows the user detection performances of some state of the art IUS algorithms for different code matrices². Note that the conventional code design procedure (see Section-IV-B) suggests using $n_{cs} = 11$. However, as can be seen in Table-I, with $u = 1$ the probability P_s of detecting a given number of codes successfully by all algorithms are uniformly poor for $n_{cs} < 15$. In contrast, P_s for both SMUD [4] and SRMD [5] are above 0.9 for $n_{cs} \geq 15$. Table-I also shows results for $u = 2$ and 3. However, comparing three different values of u , we see that the algorithms perform at their best with $u = 1$ and $n_{cs} \geq 15$. This is interesting to note that just by taking some different combinations of n_{cs} and u there is a significant variation of detection performance. Moreover, this happens uniformly for both the algorithms.

The above example clearly demonstrates the importance of choosing the parameters u and n_{cs} carefully in order to ensure that the IUS algorithms can produce the best results. To the best of our knowledge, so far, there is no systematic study in the literature addressing the issue. In the sequel, we present a systematic procedure for finding good values of u and n_{cs} that give the IUS algorithms an opportunity to perform at their best.

C. Contributions

In this work, we develop a systematic procedure to study the dependency of code detection performance of the IUS algorithms on the code matrix and demonstrate an efficient code matrix design technique. The procedure can be outlined as follows. We first develop a data model of the received signal at eNodeB over the PRACH subcarriers. We represent the received signal as a linear combination of few columns of a known matrix. This matrix is constructed by using the RA codes and some sub-Fourier matrices. We further show that the data model allows us to pose the IUS parameter estimation as a sparse signal representation problem on an overcomplete basis [15], [16]. Thereby, sparse recovery algorithms can be used for the IUS parameter estimation problem. We then apply the compressive sensing theory³ to recognize a factor that

²In case of $n_{cs} > 15$ in Table-I, we need two roots to generate the code matrix.

³Sparse recovery algorithms and theories are generally developed in the research area called ‘‘Compressive sensing’’.

controls the RA code detection performance. The factor is called ‘‘matrix coherence’’. We show that the matrix coherence of the underlying IUS problem depends on the code matrix. We then suggest a code matrix design procedure that can ensure the optimum value of matrix coherence. The simulation results clearly demonstrate that we can indeed significantly enhance the performances of the state of the art IUS parameter estimation algorithms [4], [5], [17] by using the code matrices generated by our suggested procedure. In particular, we can achieve the optimum code detection performance in Table-I by using our preferred code matrices.

II. DATA MODEL

A. Single RT

In this work, we consider the uplink data transmission protocol of an LTE-like system [6]. However, the proposed analysis can be extended for any LTE systems [1]. Consider a system with N subcarriers and N_g cyclic prefixes. Therefore, the length of an OFDM symbol is $\bar{N} = N + N_g$. Total M adjacent subcarriers are reserved for the Physical Random Access Channel (PRACH) [6]. We denote their indices by $\{j_m : m = 1, 2, \dots, M\}$. When a downlink synchronized RT wants to start communicating via the eNodeB, it must choose a column of a pre-specified $M \times G$ random access (RA) code matrix

$$\mathbf{C} = [\mathbf{c}_1^{(u_1)} \quad \mathbf{c}_2^{(u_2)} \quad \dots \quad \mathbf{c}_G^{(u_G)}] \quad (4)$$

uniformly at random, and send this code via the PRACH during a ‘‘random access opportunity’’. Note that if all RA codes are generated from same ZC root then $u_1 = u_2 = \dots = u_G$. We now mention an important property of the ZC sequence which will be helpful for developing the RA data model in the following section. One can express (2) as:

$$\mathbf{c}_{k+1, \ell+1}^{(u_\ell)} = Z^{u_\ell}(k) e^{-i2\pi u_\ell k \ell n_{cs}/M} e^{-i\pi u_\ell \ell n_{cs} (\ell n_{cs} + 1)/M} \quad (5)$$

with $0 \leq k < M$ [7], [18]. Since the index of m -th random access subcarrier is j_m , and the random access subcarriers are adjacent to each other, we have

$$j_{k+1} = j_1 + k.$$

Substituting $k = j_{k+1} - j_1$ in (5) gives

$$\mathbf{c}_{k+1, \ell+1}^{(u_\ell)} = Z^{u_\ell}(k) e^{-i2\pi u_\ell j_{k+1} \ell \frac{n_{cs}}{M}} e^{-i\pi u_\ell \ell \frac{n_{cs}}{M} (\ell n_{cs} + 1 - 2j_1)}. \quad (6)$$

Let T be a specific RT which attempts to synchronize with the eNodeB at a particular RA opportunity. In particular, T chooses the column $\mathbf{c}_\ell^{(u_\ell)}$ from \mathbf{C} and transmits it through PRACH to the eNodeB. The RT transmits $N + 2N_g$ number of time domain channel symbols which are constructed from \mathbf{c}_ℓ . We denote these $N + 2N_g$ channel symbols by $\{w(k)\}_{k=-N_g}^{N+N_g-1}$. To construct the channel symbols, at first calculate

$$s(q) = \frac{1}{\sqrt{N}} \sum_{m=1}^M \mathbf{c}_{m, \ell} \exp\{i2\pi j_m q/N\}, \quad q = \mathcal{I}, \quad (7)$$

where $\mathcal{I} := \{0, 1, 2, \dots, N - 1\}$, and $\mathbf{c}_{m, \ell}$ denotes the m th component of \mathbf{c}_ℓ . Subsequently, $\{w(k)\}_{k=-N_g}^{N+N_g-1}$ are constructed as

$$w(k) = \begin{cases} s(k \bmod N), & -N_g \leq k \leq N - 1, \\ 0, & N \leq k \leq N + N_g - 1, \end{cases} \quad (8)$$

where as usual, $(k \bmod N) := k - N \cdot \lfloor k/N \rfloor$. For any integer k positive or negative, $(k \bmod N) \in \mathcal{I}$. Note that the last N_g symbols in (8) are zero valued guard symbols [6], [19]. Note that the uplink protocol of standard LTE system [1] is slightly different than the model in (7). Standard LTE uses SC-FDMA uplink. This requires the ZC sequences first DFT pre-coded and then mapped onto subcarriers by IDFT, i.e., in (7) the $\mathbf{c}_{m, \ell}^{(u_\ell)}$ will be replaced by $\hat{\mathbf{c}}_{m, \ell}^{(u_\ell)}$ where $\hat{\mathbf{c}}_{m, \ell}^{(u_\ell)}$ its the DFT of $\mathbf{c}_{m, \ell}^{(u_\ell)}$. Nevertheless, when the length of ZC sequence is a prime number then the DFT of ZC sequence is another ZC sequence conjugated and scaled [20], [21]. As a result, the proposed analysis for ZC code in OFDMA structure is fully compliant to the SC-FDMA.

Suppose $h(p)$, $p \in \mathcal{I}$ are the uplink channel impulse response coefficients between the transmitter T and eNodeB. Let $\{v(k)\}_{k=-N_g}^{N+N_g-1}$ be the contribution of T in the symbols received by the eNodeB during the IUS opportunity. These are delayed and convoluted version of the transmitted symbols:

$$\begin{aligned} v(k) &= e^{i2\pi k \epsilon/N} \sum_{p=0}^{N-1} h(p) w(k - p - d), \quad k \in \mathcal{I} \\ &= e^{i2\pi k \epsilon/N} \sum_{p=0}^{N-1} h(p) s\{(k - p - d) \bmod N\}, \quad k \in \mathcal{I}. \end{aligned} \quad (9)$$

where delay d depends on the distance between T and eNodeB, and ϵ is the carrier frequency offset (CFO). During an uplink synchronization period, the CFO is mainly due to Doppler shifts and downlink synchronization error, they are assumed to be significantly smaller than the subcarrier frequency spacing. Hence, the impact of CFO on the initial uplink synchronization is generally neglected [3], [4], [6]. Thus $\{v(k)\}_{k=0}^{N-1}$ is the result of length N circular convolution of h , and s circularly shifted by d places. The eNodeB calculates N point discrete Fourier transform (DFT) of v to obtain

$$V(n) = \sum_{k=0}^{N-1} v(k) \exp(-i2\pi kn/N), \quad n \in \mathcal{I}. \quad (10)$$

Let S and H denote the N point DFTs of s and h , respectively. It is well known [22] that in the DFT domain the circular convolution in (9) is equivalent to

$$V(n) = H(n)S(n) \exp(-i2\pi dn/N). \quad (11)$$

Note that equation (7) is compactly given in matrix form as

$$[s(0) \quad s(1) \quad \dots \quad s(N-1)]^T = \frac{1}{\sqrt{N}} \mathbf{F}^* \mathbf{\Theta}^T \mathbf{c}_\ell^{(u_\ell)}, \quad (12)$$

where $(\cdot)^T$ and $(\cdot)^*$ denote transpose and complex conjugate transpose respectively, $\mathbf{\Theta}$ is an $M \times N$ row selector matrix which is constructed by selecting M contiguous rows from an $N \times N$ identity matrix where the first row of $\mathbf{\Theta}$ is the j_1 -th

row of the identity matrix, and the $N \times N$ DFT matrix \mathbf{F} is defined element-wise as

$$[\mathbf{F}]_{k,m} = \exp\{-i2\pi(k-1)(m-1)/N\}.$$

where $[\mathbf{F}]_{k,m}$ is the element of \mathbf{F} at its k -th row and m -th column. Thereby, the DFT of (12) is given by

$$[S(0) \ S(1) \ \cdots \ S(N-1)]^\top = \Theta^\top \mathbf{c}_\ell^{(u_\ell)}. \quad (13)$$

Using the relations in (6) and (13), and denoting $\phi_{\ell+1} = \pi u_\ell \ell n_{cs}(\ell n_{cs} + 1 - 2j_1)/M$, we can express (11) as

$$V(j_m) = Z^{u_\ell}(m)H(j_m)e^{-i\frac{2\pi}{N}j_m(u_\ell(\ell-1)n_{cs}\frac{N}{M}+d)}e^{-i\phi_\ell}. \quad (14)$$

for $m = 1, 2, \dots, M$. Note that ϕ_ℓ is known for all ℓ . After calculating V , the eNodeB forms the vector

$$\mathbf{v} = [V(j_1) \ V(j_2) \ \cdots \ V(j_M)]^\top, \quad (15)$$

From the theory of DFT, it is well known that $H(n)e^{-i2\pi dn/N}$ is the DFT of h circularly shifted by d places [22], which is written compactly as

$$\begin{aligned} & [H(0) \ H(1)e^{-i2\pi d/N} \ \cdots \ H(N-1)e^{-i2\pi d(N-1)/N}]^\top \\ &= \mathbf{F}\mathbf{h}_{\downarrow(d)}, \end{aligned} \quad (16)$$

where $\mathbf{h}_{\downarrow(d)}$ is the circularly shifted version of the channel impulse response by d places expressed as a vector:

$$\mathbf{h}_{\downarrow(d)} := [h(N-d) \ \cdots \ h(N-1) \ h(0) \ h(1) \ \cdots \ h(N-d-1)]^\top. \quad (17)$$

Hence by (16) and (17), we have

$$\begin{aligned} & [H(j_1)e^{-i\frac{2\pi}{N}j_1d} \ H(j_2)e^{-i\frac{2\pi}{N}j_2d} \ \cdots \ H(j_M)e^{-i\frac{2\pi}{N}j_Md}]^\top \\ &= \Theta \mathbf{F}\mathbf{h}_{\downarrow(d)}. \end{aligned} \quad (18)$$

Hence (14) and (15) imply that

$$\mathbf{v} = \mathbf{E}_\ell \tilde{\mathbf{h}}_{\downarrow(d)}, \quad (19)$$

$$\mathbf{E}_\ell = \text{diag}(Z^{u_\ell})\text{diag}(\mathbf{p}_\ell) \Theta \mathbf{F}. \quad (20)$$

$$\tilde{\mathbf{h}}_{\downarrow(d)} = e^{-i\phi_\ell} \mathbf{h}_{\downarrow(d)} \quad (21)$$

$$\mathbf{p}_\ell = [e^{-i\frac{2\pi}{N}j_1(u_\ell(\ell-1)n_{cs}\frac{N}{M})}, \dots, e^{-i\frac{2\pi}{N}j_M(u_\ell(\ell-1)n_{cs}\frac{N}{M})}] \quad (22)$$

where $\text{diag}(\mathbf{p}_\ell)$ denotes a diagonal matrix where the vector \mathbf{p}_ℓ is its diagonal entry. Typically, we know a number P , known as the maximum channel order [3], [4], such that $|h(k)| = 0$ for $k \geq P$. In addition, the cell radius gives an upper bound D on d . Thus, by construction of $\tilde{\mathbf{h}}_{\downarrow(d)}$, only first $D+P$ of its rows are non-zero. Hence it is fine to truncate $\tilde{\mathbf{h}}_{\downarrow(d)}$ to a $D+P$ dimensional vector, and thus it is enough to work with only first $D+P$ columns of \mathbf{E}_ℓ . By denoting $N_1 = P+D$, we can rewrite (19) as

$$\mathbf{v} = \tilde{\mathbf{E}}_\ell \tilde{\mathbf{h}}_{\downarrow(d)}(1:N_1), \quad (23)$$

where, $\tilde{\mathbf{E}}_\ell = \text{diag}(Z^{u_\ell})\text{diag}(\mathbf{p}_\ell)\Theta\mathbf{F}(:, 1:N_1)$

here $\mathbf{F}(:, 1:N_1)$ denotes the submatrix of \mathbf{F} formed by taking its first N_1 columns and $\tilde{\mathbf{h}}_{\downarrow(d)}(1:N_1)$ denotes the sub-vector of $\tilde{\mathbf{h}}_{\downarrow(d)}$ consisting of its first N_1 components. Note that $\tilde{\mathbf{E}}_\ell$ is known to the eNodeB for any ℓ . However, $\tilde{\mathbf{h}}_{\downarrow(d)}$ is unknown. In fact, the eNodeB knows neither the values of d , nor ℓ , nor the channel impulse response.

B. Multiple RTs

Let \tilde{N}_ℓ be the number of terminals transmitting code $\mathbf{c}_\ell^{(u_\ell)}$. Note that the value of \tilde{N}_ℓ can be larger than one. However, $\tilde{N}_\ell > 1$ implies that multiple RTs will collide by selecting the same RA code in a particular IUS opportunity. To prevent the collision and maintain $\tilde{N}_\ell \leq 1$, different scheduling approaches have been considered by the Third Generation Partnership Project [1]. Thus, in the following, we assume $\tilde{N}_\ell \in \{0, 1\}$. Suppose d_ℓ be the delay of the RT transmitting $\mathbf{c}_\ell^{(u_\ell)}$. Let

$$\mathbf{h}_\ell = \begin{cases} \tilde{\mathbf{h}}_{\downarrow(d_\ell)}, & \tilde{N}_\ell = 1, \\ 0, & \tilde{N}_\ell = 0. \end{cases} \quad (24)$$

Then by the principle of superposition and using (23) the data vector \mathbf{y} received by the eNodeB at the PRACH subchannels is given by

$$\mathbf{y} = \mathbf{A}\mathbf{x} + \mathbf{e}, \quad (25)$$

$$\mathbf{x} := [h_1^\top(1:N_1) \ h_2^\top(1:N_1) \ \cdots \ h_G^\top(1:N_1)]^\top,$$

$$\mathbf{A} = [\tilde{\mathbf{E}}_1 \ \tilde{\mathbf{E}}_2 \ \cdots \ \tilde{\mathbf{E}}_G].$$

where \mathbf{e} is the contribution of noise. Since $\tilde{\mathbf{E}}_\ell$ is known for any ℓ , \mathbf{A} is also known. The power received by the eNodeB corresponding to the code $\mathbf{c}_\ell^{(u_\ell)}$ is given by [3, eq. (5)]:

$$\Gamma_\ell = \frac{\sum_{m=1}^M \|\sum_{p=0}^{P-1} h_\ell(p)e^{-i2\pi pj_m/N}\|_2^2}{M}. \quad (26)$$

where $\|\mathbf{z}\|_p$ denotes the ℓ_p norm: $\|\mathbf{z}\|_p = (\sum_t |z(t)|^p)^{1/p}$.

C. IUS parameter estimation problem

Given \mathbf{y} , the eNodeB needs to *i) find the set $\mathcal{L} = \{\ell : \Gamma_\ell \neq 0\}$; and *ii) for every $\ell \in \mathcal{L}$ find Γ_ℓ and d_ℓ .**

Recall that the first d components of $\mathbf{h}_{\downarrow(d)}$ are zero, see (17). Hence by construction of \mathbf{h}_ℓ in (24), the index of the first nonzero component of \mathbf{h}_ℓ is $1+d_\ell$. This observation can be used to find d_ℓ from an estimate of \mathbf{h}_ℓ .

III. IUS PARAMETER ESTIMATION AS A SPARSE SIGNAL RECOVERY PROBLEM

By construction, $\mathbf{A} \in \mathbb{C}^{M \times G \cdot N_1}$ in (25) is a known matrix. On the other hand, \mathbf{x} and \mathbf{e} are unknowns and we have to obtain an estimate of \mathbf{x} to resolve the IUS problem. Typically, the total number of RTs $K = \sum_{\ell=1}^G \tilde{N}_\ell \ll G$, implying $\tilde{N}_\ell = 0$ (and therefore $\mathbf{h}_\ell = 0$) for a vast majority of the values $\ell \in \{1, 2, \dots, G\}$. This makes \mathbf{x} very sparse, motivating a sparse recovery approach for solving the IUS problem.

Suppose we obtain a sparse estimate $\check{\mathbf{x}}$ of \mathbf{x} by applying a sparse recovery algorithm on (25). From the estimate $\check{\mathbf{x}}$, the eNodeB can extract the IUS information as follows. Partition $\check{\mathbf{x}}$ into G sub-vectors:

$$\check{\mathbf{x}} = [\check{\mathbf{h}}_1^\top \ \check{\mathbf{h}}_2^\top \ \cdots \ \check{\mathbf{h}}_G^\top]^\top,$$

where each $\check{\mathbf{h}}_\ell$ is of length N_1 . Then we declare $\ell \in \mathcal{L}$ only if $\|\check{\mathbf{h}}_\ell\|_2 \neq 0$ and the index of the first nonzero component of $\check{\mathbf{h}}_\ell$ leads to an estimate of d_ℓ .

A. Performance of sparse recovery algorithm for resolving the IUS problem

To observe the IUS parameter estimation performance by using a sparse recovery algorithm, we apply a popular approach called least absolute shrinkage and selection operator (Lasso) [23], [24]. Using the Lasso paradigm, we need to solve the following optimization problem:

$$\mathbf{x}_* = \arg \min_{\mathbf{z}} \lambda \|\mathbf{z}\|_1 + \frac{1}{2} \|\mathbf{A}\mathbf{z} - \mathbf{y}\|_2^2 \quad (27)$$

where the value of $\lambda > 0$ depends on the noise level. The typical results of IUS parameter estimation by using the Lasso with similar setup in Table-I has been demonstrated in Table-II. Similar to the state of the art IUS algorithms, the performance of Lasso also depends on the code matrix. In fact, when SMUD and SRMD perform well, Lasso also performs well. On the other hand, for the selection of code matrices leading to performance deterioration of the SMUD and SRMD, Lasso also shows very clear deterioration of performance. This observation inspires us to investigate the dependency of algorithms performance on the code matrix by using the compressive sensing theory⁴.

B. The coherence parameter

In general, the performance of sparse recovery algorithms depends on some properties of the matrix \mathbf{A} . Two types of metric are commonly used to characterize the properties of a matrix: i) restricted isometry property (RIP) [25], [26] and (ii) mutual coherence [24], [27]. A matrix satisfying the restricted isometry property will approximately preserve the length of all signals up to a certain sparsity, thereby, provides performance guaranty of sparse recovery algorithms. However, evaluating the RIP of a matrix is a computationally hard problem in general [28]. On the other hand, computing mutual coherence of a matrix is easy. In this respect, the coherence based results of performance guaranty of sparse recovery algorithms are appealing since they can be evaluated easily for any arbitrary matrix. In this work, we seek the performance guarantee of sparse recovery algorithms based on the mutual coherence.

The ‘‘mutual coherence’’ $\mu(\mathbf{A})$ of \mathbf{A} is defined as [24]

$$\mu(\mathbf{A}) = \max_{i \neq j} \frac{|[\mathbf{A}]_i^* [\mathbf{A}]_j|}{\|[\mathbf{A}]_i\|_2 \|[\mathbf{A}]_j\|_2}, \quad (28)$$

where $[\mathbf{A}]_i$ denotes the i -th column of \mathbf{A} and $[\mathbf{A}]_i^*$ is its complex conjugate transpose. In particular, the coherence is defined as the maximum absolute value of the cross-correlations between the normalized columns of \mathbf{A} . When the coherence is small, the columns look very different from each other, which makes them easy to distinguish. Thereby, it is used as a measure of the ability of sparse recovery algorithms to correctly identify the true representation of a sparse signal [29]. The theoretical results in [24], [27] show that the performance of a sparse recovery algorithm can be improved by minimizing $\mu(\mathbf{A})$. We validate this theoretical result for IUS application in Table-II where we list the values

⁴Sparse recovery algorithms and theories are generally developed in the research area called ‘‘Compressive sensing’’.

of $\mu(\mathbf{A})$ for different ZC root u and n_{cs} . By comparing those values of $\mu(\mathbf{A})$ with the P_s of Lasso, we see that the performance of Lasso increases with decreasing the value of $\mu(\mathbf{A})$. Thereby, we can improve the performance of Lasso by minimizing the value of $\mu(\mathbf{A})$. In the following section, we show that the value of $\mu(\mathbf{A})$ can be controlled by properly designing the code matrix.

IV. SINGLE ROOT CODE MATRIX DESIGN

In this section, we derive an expression for $\mu(\mathbf{A})$ by assuming that all codes in the code matrix \mathbf{C} are generated from the same ZC root, i.e., we assume that $u_\ell = \tilde{u}; \forall \ell \in \{1, 2, \dots, G\}$ in (4). Consequently, we propose a code matrix design procedure that can ensure the optimum value of $\mu(\mathbf{A})$. In the next section, we extend the code matrix design procedure for multiple roots.

A. Coherence of \mathbf{A} for single root

The following lemma gives the coherence property of \mathbf{A} .

Lemma 1: Assume that $u_\ell = \tilde{u}; \forall \ell \in \{1, 2, \dots, G\}$ in (4). Furthermore, $\pi\sqrt{2} \leq M \leq N/2$. Then it holds that

$$\mu(\mathbf{A}) = \left| \frac{\text{sinc}(g(\tilde{u})M/N)}{\text{sinc}(g(\tilde{u})/N)} \right|, \quad (29)$$

where $\text{sinc}(x) = \sin(\pi x)/(\pi x)$ and $g(\tilde{u}) = \min\{1, \zeta(\tilde{u})\}$. Here we define

$$\zeta(\tilde{u}) := \min_{\substack{\ell \neq m \\ 1 \leq p, k \leq N_1}} \left\{ \left(\frac{n_{cs} \tilde{u} N}{M} (\ell - m) + (p - k) \right) \bmod N \right\} \quad (30)$$

with $m, \ell \in \{1, 2, \dots, G\}$.

Proof: See Appendix-A. ■

In a typical LTE system [6] the values of $M = 839$ and $N = 6144$. Therefore, the assumption of Lemma-1 i.e., $\pi\sqrt{2} \leq M \leq N/2$ holds in practice. Under the assumptions of Lemma-1, the value of $\mu(\mathbf{A})$ is the smallest when $g(\tilde{u}) = 1$. If the value of $\zeta(\tilde{u})$ becomes smaller than one then it will increase the value of matrix coherence. The code design procedure proposed here will aim to maintain $\zeta(\tilde{u}) \geq 1$.

In this following sections, we first demonstrate the conventional procedure of code matrix design. We show that the procedure may not achieve the minimum value of coherence of \mathbf{A} . Finally, we demonstrate an efficient code matrix design procedure.

B. Conventional procedure of generating RA code matrix (CRA)

The conventional procedure of generating RA code sequences has been described in [1], [14]. For the given specification of an LTE system, we need to compute the smallest integer for n_{cs} that satisfies (3). For a given specification of the LTE system, we take \hat{n}_{cs} as the smallest integer satisfying (3). Set $n_{cs} = \hat{n}_{cs}$ and compute $G = \lfloor M/n_{cs} \rfloor$ which is the maximum number of codes that can be generated from a single root. We then choose an arbitrary non-zero positive

TABLE II

IUS USER DETECTION PROBABILITIES BY LASSO AND MUTUAL COHERENCE OF \mathbf{A} FOR DIFFERENT VALUES OF u AND n_{cs} . SNR=10 dB, TOTAL IUS USERS $K = 3$ AND P_s DENOTES THE PROBABILITY OF SUCCESSFULLY DETECTING THE USERS.

	ZC root $u = 1$					ZC root $u = 2$		
	$n_{cs} = 11$	13	15	17	19	$n_{cs} = 11$	13	17
P_s	0.71	0.7	0.99	0.99	0.99	0.27	0.68	0.71
$\mu(\mathbf{A})$	0.994	0.998	0.969	0.969	0.969	1.0	0.998	0.993

integer for the root \tilde{u} such that $\tilde{u} < M$ [1]. Subsequently, we generate G number of RA codes $\{\mathbf{c}_\ell\}_{\ell=1}^G$ by using (2). However, this procedure may produce a code matrix \mathbf{A} with bad value of $\mu(\mathbf{A})$. Such examples are readily constructed. Consider the LTE system with $N = 6144$, $N_g = 768$ and $M = 839$ and OFDM symbol sampling interval is 130 ns. The cell radius $\gamma = 1.5$ km and $N_1 = 105$. Using (3), we obtain a lower bound $\hat{n}_{cs} = 13$. Suppose we want to generate total 50 codes. By using those values, we construct a code matrix \mathbf{C} by applying the above procedure where we set $\tilde{u} = 1$. We found that $\zeta(1) = 0.199$ and consequently $\mu(\mathbf{A}) = 0.9988$.

C. Coherence based code generation (CCG)

Recall that the minimum value of $\mu(\mathbf{A})$ in (29) can be obtained by making $\zeta(\tilde{u}) \geq 1$, i.e., for every $p, k \in \{1, 2, \dots, N_1\}$ and $\ell, m \in \{1, 2, \dots, G\}$ with $\ell \neq m$, we have to satisfy

$$\left\{ \left(\frac{n_{cs} \tilde{u} N}{M} (\ell - m) + (p - k) \right) \bmod N \right\} \geq 1. \quad (31)$$

The following proposition gives a sufficient condition to fulfill the requirement in (31).

Proposition 1: If

$$N_1 \leq \frac{n_{cs} \tilde{u} N}{M} \leq \frac{N - N_1}{G - 1}, \quad (32)$$

then (31) holds for every $p, k \in \{1, 2, \dots, N_1\}$ and $\ell, m \in \{1, 2, \dots, G\}$ with $\ell \neq m$.

Proof: It is sufficient to show that if (32) holds then

$$1 \leq \left| \frac{n_{cs} \tilde{u} N}{M} (\ell - m) + (p - k) \right| \leq N - 1 \quad (33)$$

for any $p, k \in \{1, 2, \dots, N_1\}$ and $\ell, m \in \{1, 2, \dots, G\}$ with $\ell \neq m$.

Suppose that (32) holds. Then using reverse triangle inequality [30], we see that

$$\begin{aligned} & \left| \frac{n_{cs} \tilde{u} N}{M} (\ell - m) + (p - k) \right| \\ & \geq \left| \frac{n_{cs} \tilde{u} N}{M} (\ell - m) \right| - |(p - k)| \\ & \geq \frac{n_{cs} \tilde{u} N}{M} - (N_1 - 1) \\ & \geq 1 \end{aligned} \quad (34)$$

where the last inequality follows from the first inequality of (32).

TABLE III

COHERENCE BASED CODE GENERATION (CCG) FOR SINGLE ZC ROOT

Input: The value of \hat{n}_{cs} and a ZC root \tilde{u} .

Initialization: Set \mathbf{C} is empty.

1. Find the smallest positive integer n_{cs} such that $\hat{n}_{cs} \leq n_{cs}$ and satisfies lower bound of (32) i.e., $\frac{M N_1}{N} \leq n_{cs} \tilde{u}$.
2. Compute G using (36): $G = \lfloor 1 + \frac{M(N - N_1)}{N n_{cs} \tilde{u}} \rfloor$.
3. **For** $\ell = 1 : G$
4. Generate $\mathbf{c}_\ell^{(\tilde{u})}$ using (2).
5. Update $\mathbf{C} = [\mathbf{C} \ \mathbf{c}_\ell^{(s)}]$.
6. **End for.**

7. Output: Code matrix \mathbf{C} .

On the other hand, triangle inequality implies

$$\begin{aligned} & \left| \frac{n_{cs} \tilde{u} N}{M} (\ell - m) + (p - k) \right| \\ & \leq \left| \frac{n_{cs} \tilde{u} N}{M} (\ell - m) \right| + |(p - k)| \\ & \leq \frac{n_{cs} \tilde{u} N (G - 1)}{M} + (N_1 - 1) \\ & \leq N - N_1 - N_1 + 1 = N - 1 \end{aligned} \quad (35)$$

where we use the second inequality of (32). Combining (34) and (35) we get (33). ■

Remark 1: Note that for some given values of n_{cs} and \tilde{u} , eq. (32) gives an upper bound on the maximum number of codes that can be generated i.e.,

$$G \leq 1 + \frac{M(N - N_1)}{N n_{cs} \tilde{u}}. \quad (36)$$

Table-III shows the proposed CCG algorithm. Here \hat{n}_{cs} denotes the value of lower bound of n_{cs} that satisfies (3). Unlike the CRA algorithm (Section-IV-B), we do not use the value of \hat{n}_{cs} directly for code generation. Instead, we use \hat{n}_{cs} to choose an appropriate value of n_{cs} in Step-1 which satisfies the lower bound in (32). Given n_{cs} , we use (36) to compute the value of G in Step-2. Subsequently, the algorithm generates G number of codes using Step-3 to Step-6.

V. MULTIPLE ROOT CODE MATRIX DESIGN

In practice, the code matrix \mathbf{C} in (4) can be generated by using multiple ZC roots. We denote \mathcal{U} as the set of all roots that has been used to generate \mathbf{C} i.e. $u_\ell \in \mathcal{U}; \forall \ell \in \{1, 2, \dots, G\}$. Let \mathcal{J}_u be the set of all column indices of \mathbf{C} that are generated from the root u . To give an example, assume that \mathbf{C} has been generated from the two roots $\{1, 2\}$, where the first 3 columns of \mathbf{C} are generated using root number 1. Hence, $\mathcal{U} := \{1, 2\}$

and $\mathcal{J}_1 := \{1, 2, 3\}$. Hence, in (4) we have $u_\ell = 1; \ell = 1, 2, 3$ and $u_\ell = 2; \ell = 4, \dots, G$. Thus, in this case

$$\mathbf{C} = [\mathbf{c}_1^{(1)} \quad \mathbf{c}_2^{(1)} \quad \mathbf{c}_3^{(1)} \quad \mathbf{c}_4^{(2)} \quad \dots \quad \mathbf{c}_G^{(2)}].$$

Let \mathbf{B}_u be the matrix which is constructed by concatenating the matrices $\tilde{\mathbf{E}}_\ell; \ell \in \mathcal{J}_u$. For example, if the first three columns of \mathbf{C} are generated from the root u then $\mathcal{J}_u := \{1, 2, 3\}$ and $\mathbf{B}_u = [\tilde{\mathbf{E}}_1 \quad \tilde{\mathbf{E}}_2 \quad \tilde{\mathbf{E}}_3]$. In this way, we can view \mathbf{A} as a concatenation of matrices $\mathbf{B}_u; u \in \mathcal{U}$.

To derive an expression for $\mu(\mathbf{A})$, we require the following definition. For any two matrices $\mathbf{U} \neq \mathbf{D}$, we extend the definition of mutual coherence in (28) to ‘‘block coherence’’ as

$$\hat{\mu}(\mathbf{U}, \mathbf{D}) = \max_{j,k} \frac{|[\mathbf{U}]_j^* [\mathbf{D}]_k|}{\|[\mathbf{U}]_j\|_2 \|[\mathbf{D}]_k\|_2}. \quad (37)$$

where $[\mathbf{D}]_k$ denotes the k -th column of \mathbf{D} . Therefore

$$\mu(\mathbf{A}) = \max_{p \in \mathcal{U}} \left\{ \max_{u_1 \neq u_2; u_1, u_2 \in \mathcal{U}} \hat{\mu}(\mathbf{B}_{u_1}, \mathbf{B}_{u_2}) \right\}. \quad (38)$$

In the following, we develop a code design procedure so that we can maintain $\mu(\mathbf{A})$ to its minimum value i.e.,

$$\mu(\mathbf{A}) = \left| \frac{\text{sinc}(M/N)}{\text{sinc}(1/N)} \right|. \quad (39)$$

We assume that the following condition holds for any $p \in \mathcal{U}$

$$\mu(\mathbf{B}_p) = \left| \frac{\text{sinc}(M/N)}{\text{sinc}(1/N)} \right|. \quad (40)$$

In particular, we can satisfy (40) by constructing \mathbf{B}_p using the CCG method in Section-IV-C. Next, we see that

$$\max_{u_1 \neq u_2; u_1, u_2 \in \mathcal{U}} \hat{\mu}(\mathbf{B}_{u_1}, \mathbf{B}_{u_2}) = \max_{\substack{\ell \in \mathcal{J}_{u_1}; m \in \mathcal{J}_{u_2} \\ u_1 \neq u_2; u_1, u_2 \in \mathcal{U}}} \hat{\mu}(\tilde{\mathbf{E}}_\ell, \tilde{\mathbf{E}}_m). \quad (41)$$

It is difficult to develop an exact expression for (41). Nevertheless, we provide an upper bound for the value of (41). By using the definition of block coherence in (37), we get

$$\hat{\mu}(\tilde{\mathbf{E}}_\ell, \tilde{\mathbf{E}}_m) = \max_{1 \leq k, p \leq N_1} \frac{1}{M} |[\tilde{\mathbf{E}}_\ell]_k^* [\tilde{\mathbf{E}}_m]_p|. \quad (42)$$

Next we give an upper bound on the right hand side of (42).

Proposition 2: For any $k, p \in \{1, 2, \dots, N_1\}$ with $\ell \in \mathcal{J}_{u_1}; m \in \mathcal{J}_{u_2}; u_1, u_2 \in \mathcal{U}$ and $u_1 \neq u_2$, it holds that

$$\begin{aligned} & \frac{1}{M} |[\tilde{\mathbf{E}}_\ell]_k^* [\tilde{\mathbf{E}}_m]_p| \\ &= \frac{1}{M} \left| \sum_{n=0}^{M-1} \exp \left\{ -i \frac{\pi}{M} (u_2 - u_1) \right. \right. \\ & \quad \left. \left. \{n + \vartheta(u_1, u_2, \ell, m, p, k)\}^2 \right\} \right| \end{aligned} \quad (43)$$

where, $\vartheta(u_1, u_2, \ell, m, p, k)$

$$= \frac{1}{2} + \frac{1}{(u_2 - u_1)} \left\{ n_{cs} (u_2(m-1) - u_1(\ell-1)) + (p-k) \frac{M}{N} \right\}. \quad (44)$$

Proof: See Appendix-C. \blacksquare

Lemma 2: Suppose the following conditions hold for some $k, p \in \{1, 2, \dots, N_1\}$ with $\ell \in \mathcal{J}_{u_1}; m \in \mathcal{J}_{u_2}$ and $u_1 \neq u_2$:

- C1. M is an odd prime integer.
- C2. $(u_2 - u_1)$ is an even integer.
- C3. $\vartheta(u_1, u_2, \ell, m, p, k)$ is integer valued.

Then the following relation holds

$$\frac{1}{M} |[\tilde{\mathbf{E}}_\ell]_k^* [\tilde{\mathbf{E}}_m]_p| = \frac{1}{\sqrt{M}}. \quad (45)$$

Proof: Under conditions C1-C3, the sequence

$$z(n) = \exp \left(-i \frac{\pi}{M} (u_2 - u_1) \{n + \vartheta(u_1, u_2, \ell, m, p, k)\}^2 \right) \quad (46)$$

with $n = 0, 1, 2, \dots, M-1$ satisfies $|\sum_{n=0}^{M-1} z(n)| = \sqrt{M}$ [31]. Thereby, (45) holds. \blacksquare

Remark 2: Under conditions C1-C3 of Lemma-2, the sequence $z(n)$ (defined in (45)) is known as the Frank-Zadoff-Chu (FZC) sequence [7], [8], [31].

Note that in LTE system $M = 839$. Thus, the first condition of the Lemma-2 holds. Furthermore, we can fulfill the second condition by appropriately choosing the ZC root sequences. However, the third condition may not hold for all $k, p \in \{1, 2, \dots, N_1\}$. We observe that $|\sum_{n=0}^{M-1} z(n)| \approx \sqrt{M}$, whenever $\vartheta(u_1, u_2, \ell, m, p, k)$ is approximately an integer. In practice, the value of (43) remains close to $1/\sqrt{M}$ for any feasible value of $\vartheta(u_1, u_2, \ell, m, p, k)$ defined in (44). Furthermore, for a typical LTE system ($M = 839, N = 6144$)

$$\frac{1}{\sqrt{M}} \ll \left| \frac{\text{sinc}(M/N)}{\text{sinc}(1/N)} \right|.$$

Hence,

$$\max_{\substack{\ell \in \mathcal{J}_{u_1}; m \in \mathcal{J}_{u_2} \\ u_1 \neq u_2; u_1, u_2 \in \mathcal{U}}} \hat{\mu}(\tilde{\mathbf{E}}_\ell, \tilde{\mathbf{E}}_m) \leq \left| \frac{\text{sinc}(M/N)}{\text{sinc}(1/N)} \right| \quad (47)$$

holds with high probability, and thus we should be able to find roots u_1 and u_2 satisfying (39). Nevertheless, to be more precise, we develop a systematic procedure to choose the ZC roots so that (39) holds.

The root selection problem can be described formally in the following way. Suppose, total t number of columns of \mathbf{C} have already been generated from the set of roots \mathcal{U} such that (39) is satisfied. Given \mathcal{U} and $\mathcal{J}_{u_1}; u_1 \in \mathcal{U}$ we need to choose another root u_2 and generate additional columns of \mathbf{C} so that (39) holds.

Note that for some given values of u_2 and n_{cs} satisfying the lower bound of (32), we can generate maximum $G_{u_2} = \lfloor \frac{M(N-N_1)}{N n_{cs} u_2} + 1 \rfloor$ number of columns of \mathbf{C} (see (36)). Denote $\mathcal{J}_{u_2} = \{t+1, t+2, \dots, t+G_{u_2}\}$. Since the columns are generated by satisfying (32), we have

$$\mu(\mathbf{B}_r) = \left| \frac{\text{sinc}(M/N)}{\text{sinc}(1/N)} \right|.$$

TABLE IV
COHERENCE BASED CODE GENERATION (CCG) FOR MULTIPLE ZC ROOT

Input: The value of G and the value of \hat{n}_{cs} .

Initialization: Set \mathbf{C} is empty, \mathcal{U} is empty, $u = 1$ and $t = 0$.

repeat

1. Find the smallest positive integer n_{cs} such that $\hat{n}_{cs} \leq n_{cs}$ which satisfies lower bound of (32) i.e., $\frac{MN_1}{N} \leq n_{cs}u$.
2. Compute G_u using (36): $G_u = \lfloor 1 + \frac{M(N-N_1)}{Nn_{cs}u} \rfloor$.
3. Set $\mathcal{J}_u := \{t+1, t+2 \dots t+G_u\}$.
4. If the condition in (48) does not satisfy then goto Step 12.
5. **For** $\ell = 1 : G_u$
6. Generate $\mathbf{c}_\ell^{(u)}$ using (2).
7. Update $\mathbf{C} = [\mathbf{C} \ \mathbf{c}_\ell^{(u)}]$.
8. $t = t + 1$.
9. If $t = G$ then goto Step 13.
10. **End for**.
11. Set $\mathcal{U} := \{\mathcal{U}, u\}$.
12. $u = u + 1$.

Continue to Step 1.

13. Output: Code matrix \mathbf{C} .

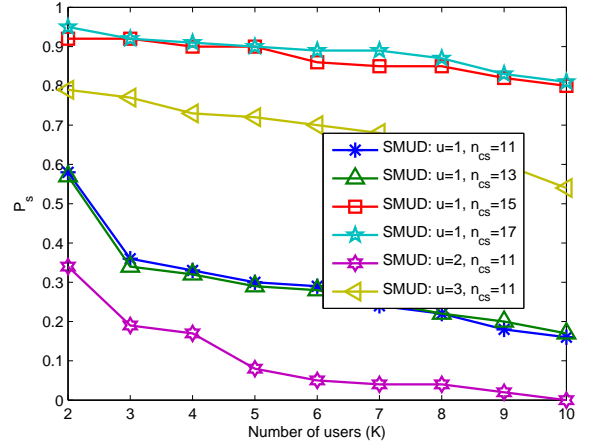
Then according to Proposition-2, it is sufficient to check

$$\max_{\substack{p, k \in \{1, 2, \dots, N_1\} \\ m \in \mathcal{J}_{u_2}, \ell \in \mathcal{J}_{u_1}; \forall u_1 \in \mathcal{U}}} \frac{1}{M} \left| \sum_{n=0}^{M-1} \exp\left(-i \frac{\pi}{M}(u_2 - u_1)n\right) \{n + \vartheta(u_1, u_2, \ell, m, p, k)\}^2 \right| \leq \left| \frac{\text{sinc}(M/N)}{\text{sinc}(1/N)} \right|. \quad (48)$$

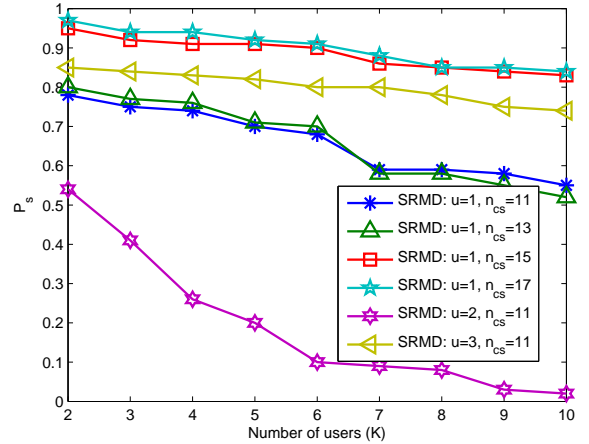
Based on the idea, the multiple root code matrix generation procedure has been described in Table-IV. Suppose that we want to generate total G number of codes. The algorithm initiates with the ZC root $u = 1$. Given the value of u , and \hat{n}_{cs} as the lower bound of n_{cs} , we compute the values of n_{cs} in Step 1 and G_u in Step-2. In Step-4, we check that whether the condition in (48) is satisfied. If the condition is satisfied then we concatenate G_u number of codes for \mathbf{C} in Step-5 to Step-10. In Step-11, we add the active root u with the set \mathcal{U} .

VI. SIMULATION RESULTS

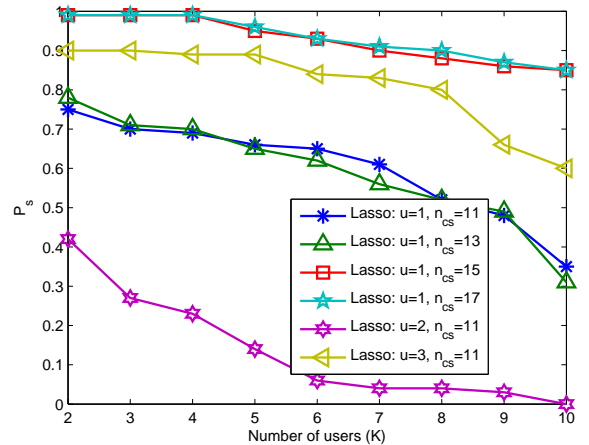
We simulate an LTE system similar to [6] where $N = 6144$, and cyclic prefix length $N_g = 768$. The subcarrier frequency spacing is 1.25 kHz, and the sampling interval $T_s = 130$ ns. The PRACH consist of $M = 839$ adjacent subcarriers. The wireless cell radius is 1.3 km, which corresponds to $D = 70$. The wireless channels are modeled according to a mixed channel model specified by the ITU IMT-2000 standards: Ped-A, Ped-B, and Veh-A. For each RT, the simulator selects one of the above channel models uniformly at random. The mobile speed varies in the interval $[0, 5]$ m/s for Ped-A, Ped-B channels, and $[5, 20]$ m/s for Veh-A. The channel impulse response of the RTs have a maximum order of $P_{\max} = 35$ taps [6]. Similar to [3], [4], we assume that eNodeB has an approximate knowledge about P_{\max} , and we set $N_1 = P_{\max} + D$ in (23). The RA codes are the Zadoff-Chu (ZC) sequences of length 839. The lower bound of n_{cs} for the ZC sequence is



(a) SMUD [4]



(b) SRMD [5]



(c) Lasso

Fig. 1. Code detection performance as a function of number of users for different values of ZC root u and n_{cs} . Signal SNR=10 dB. The CRA matrices are generated with $n_{cs} \in \{11, 13\}$ and $u \in \{1, 2, 3\}$. The CCG matrices are generated using $n_{cs} \in \{15, 17\}$ and $u = 1$.

calculated by using (3), and we get $n_{cs} \geq 11$. The number G of available RA codes in the matrix \mathbf{C} for contention based random access is 50. Recall that, at a particular random access opportunity, the set of active RA code indices is \mathcal{L} . Let $\hat{\mathcal{L}}$ be the set of code indices detected by an algorithm. The probability that $\mathcal{L} = \hat{\mathcal{L}}$, denoted by P_s , is used to quantify the merit of the algorithm [32]. The signal to noise ratio (SNR) is defined as $\text{SNR} = 10 \log_{10}(\sigma_h^2/\sigma_e^2)$, where σ_h^2 is the variance of a channel tap, and σ_e^2 is the variance of a component of \mathbf{e} , respectively [3]. For the Lasso algorithm in (27), we set $\lambda = \sqrt{8\sigma_e^2(1+\alpha)\ln(G.N_1)}$ [27], where $\alpha = 4$. The following results are based on 200 independent Monte-Carlo simulations.

In Figure-1, we compare the code detection performance of different algorithms with different code matrices generated by the CRA and CCG methods. For the LTE configuration under consideration, the conventional code matrix generation procedure i.e., CRA method (see Section-IV-B) suggests using $n_{cs} = 11$ and we can set the value of ZC root arbitrarily. Hence, we choose three different values of ZC root i.e., $u \in \{1, 2, 3\}$ to illustrate performance of the IUS algorithms. In contrast, the CCG method, described in Section-IV-C, suggests using $u = 1$ and $n_{cs} \geq 15$. Thus, we use two different values of $n_{cs} \in \{15, 17\}$. Note that we apply the multiple root CCG method (Table-IV) for code generation whenever $n_{cs} \geq 17$. As can be seen in Figure-1, the code detection probability of any particular algorithm remains almost similar for any value of $n_{cs} \in \{15, 17\}$ with $u = 1$. However, a larger value of n_{cs} decreases the value of G_u (see (36)), that is the maximum number of codes that can be generated from the single root u with the CCG algorithm. Hence, we shall use $n_{cs} = 15$ for CCG algorithm in the following experiments. As can be seen, all algorithms exhibit their optimum performances with the CCG code matrices. For example, the code detection probabilities of SMUD algorithm in Figure-1(a) are 0.92 and 0.8 with the CCG matrix ($n_{cs} = 15$) for 2 and 10 users respectively. In contrast, SMUD exhibits different types of performance for three different values of u with the CRA matrices. The code detection probabilities remain 0.6, 0.35 and 0.78 with 2 users for $n_{cs} = 11$ and $u = 1, 2$ and 3 respectively. As expected the performance deteriorates with the increase in the number of users. With 10 users, the P_s are 0.17, 0.01 and 0.54 respectively for $n_{cs} = 11$ and $u = 1, 2$ and 3. The SRMD algorithm in Figure-1(b) also shows similar performance with the code matrices. We have stated in Section-III that the code detection problem can be solved by using a sparse recovery algorithm. The results in Figure-1(c) justify our claim. Similar to the state of the art IUS algorithms, the Lasso can detect RA codes efficiently. To illustrate the robustness of the IUS algorithms with the CCG matrix in noisy environment, we present Figure-2, where we evaluate the code detection performance of IUS algorithms in relatively lower SNR. As can be seen, the algorithms still perform better with the CCG code matrix.

We examine the miss-detection probability P_{md} of different IUS algorithms for different code matrices in Figure-3. Here ‘miss-detection’ occurs when an algorithm includes the index of an inactive code into $\hat{\mathcal{L}}$. As can be seen the miss-detection

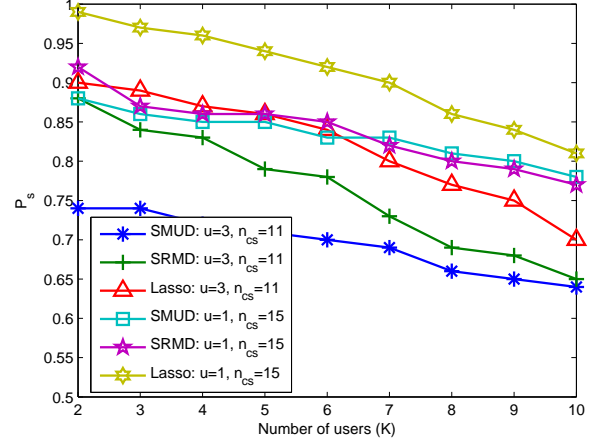


Fig. 2. Code detection performance by different algorithms at SNR=5 dB. The CRA matrix is generated with $n_{cs} = 11$ and $u = 3$. The CCG matrix is generated using $n_{cs} = 15$ and $u = 1$.

probability of all IUS algorithms are higher with the CRA matrix compared to the CCG matrix. For example, with 6 users the miss-detection probability of Lasso are 0.08 and 0.03 for CRA and CCG code matrices respectively. The miss-detection probability increases with increasing the number of active users. With 9 users, the miss-detection probability of Lasso are 0.23 and 0.1 respectively for CRA and CCG code matrices. Both SMUD and SRMD algorithms also perform similarly.

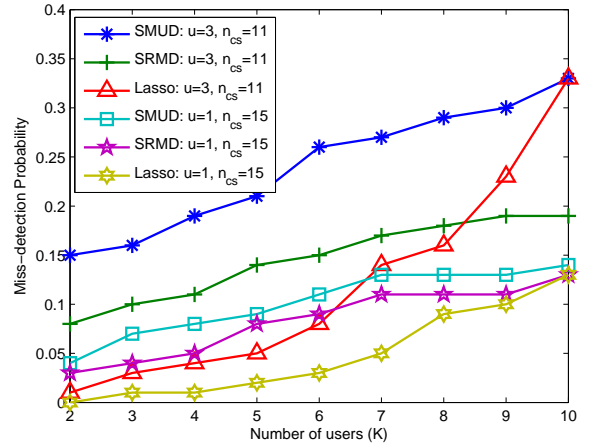


Fig. 3. Miss-detection probability by different IUS algorithms at SNR=10 dB. The CRA matrix is generated with $n_{cs} = 11$ and $u = 3$. The CCG matrix is generated using $n_{cs} = 15$ and $u = 1$.

In Figure-4 we plot the mean squared error (MSE) associated with the estimate of the power Γ and timing offset as a function of K for different code matrices. As expected, the MSE of power estimate by different algorithms is better with the CCG code matrix compared to the CRA matrix. It is interesting to note that the power estimation performance of the Lasso is poor for CRA matrix, however, it performs the best compared to other algorithms when we use the CCG matrix. Figure-4 (b) also exhibits that we can enhance

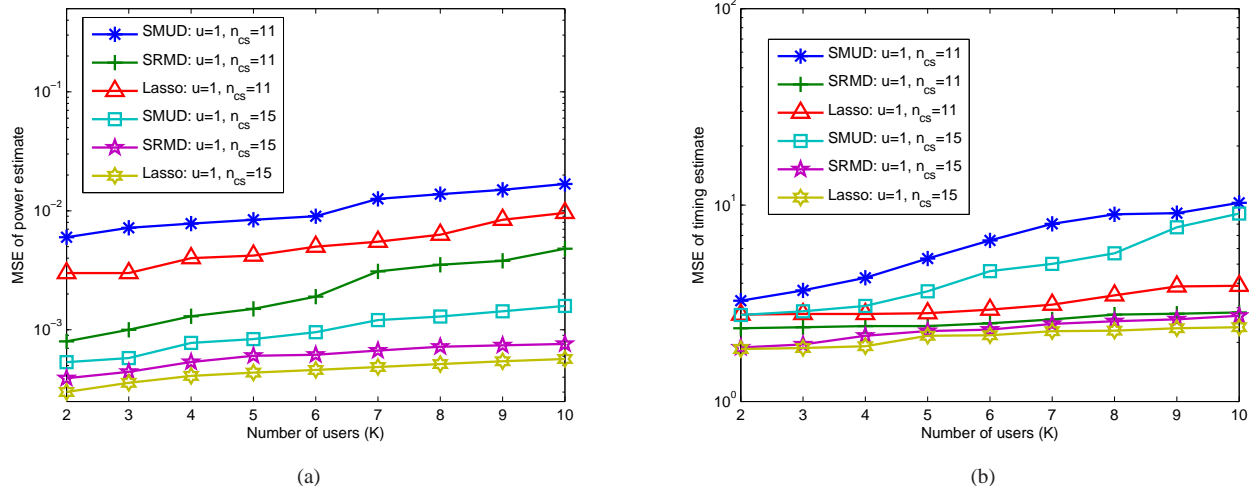


Fig. 4. MSE of initial uplink synchronization parameter estimations. (a) MSE of estimated channel power versus the number of active RTs, (b) MSE of estimated timing offset versus the number of active RTs. SNR=10 dB. The CRA matrix is generated with $n_{cs} = 11$ and $u = 1$. The CCG matrix is generated using $n_{cs} = 15$ and $u = 1$.

the timing estimate performance of different algorithms by applying the proposed code matrix.

VII. CONCLUSION

In this work, we study the dependency of performance of some state-of-the-art initial uplink synchronization algorithms on the random access (RA) code matrix which has been generated from the Zadoff-Chu (ZC) sequences. We observe that the algorithms can not perform equally for all ZC sequences. To identify the efficient ZC sequences, we apply a theory of compressive sensing. At first we develop a data model of the received signal at eNodeB over the PRACH. The data model allows us pose the IUS problem as a sparse signal representation problem on an overcomplete matrix. Consequently, we apply a sparse recovery algorithm for resolving the IUS problem. The compressive sensing theory says that the performance of sparse recovery algorithm depends on a property of the overcomplete matrix called “mutual coherence” where a smaller value of the mutual coherence ensures better performance of the algorithm. We show that the value of mutual coherence can be controlled by properly designing the RA code matrix. We then develop a systematic procedure of code matrix design which ensures the optimum value of coherence. The empirical results show that if we design the code matrix by using the proposed method then it also increases the performance of state of the art IUS algorithms. In particular, compared to conventional code matrix, the IUS algorithms with the proposed code matrix show significant performance improvements in the multiuser code detection, timing offset and channel power estimations.

APPENDIX A PROOF OF THE LEMMA-1

We begin the proof by describing some important properties of the sinc function. Define

$$\mathcal{S}(r) = \left| \frac{\text{sinc}(rM/N)}{\text{sinc}(r/N)} \right|. \quad (49)$$

For any value of $|r| < \infty$,

$$\mathcal{S}(r) = \mathcal{S}(N - r), \quad (50)$$

$$\mathcal{S}(r) = \mathcal{S}(r \bmod N). \quad (51)$$

We have shown in Appendix-B that for $\pi\sqrt{2} \leq M \leq N/2$, the $\mathcal{S}(r)$ also satisfies the following properties:

- 1) $\mathcal{S}(r)$ is a monotonically decreasing function for $r \in [0, 1]$,
- 2) for $r \in [1, N-1]$, the maximizer of $\mathcal{S}(r)$ is unique and is given by

$$\arg \max_{1 \leq r < N-1} \mathcal{S}(r) = 1. \quad (52)$$

We are now ready to prove Lemma-1. For any two matrices $\mathbf{B} \neq \mathbf{D}$, we extend the definition of mutual coherence in (28) to “block coherence” as

$$\hat{\mu}(\mathbf{B}, \mathbf{D}) = \max_{j,k} \frac{|[\mathbf{B}]_j^* [\mathbf{D}]_k|}{\|[\mathbf{B}]_j\|_2 \|[\mathbf{D}]_k\|_2}. \quad (53)$$

By using the definitions of coherences in (28) and (53), it can be verified that

$$\mu(\mathbf{A}) = \max\{\mu(\tilde{\mathbf{E}}_1), \max_{\ell \neq m} \hat{\mu}(\tilde{\mathbf{E}}_m, \tilde{\mathbf{E}}_\ell)\}. \quad (54)$$

Since all codes of \mathbf{C} are generated from the single ZC root \tilde{u} , by using (20) we have

$$[\tilde{\mathbf{E}}_m]_{q,k} = Z^{\tilde{u}}(q) \exp\left(\frac{-i2\pi j_q}{N} \left((m-1)\frac{n_{cs} \tilde{u} N}{M} + (k-1)\right)\right) \quad (55)$$

where $[\tilde{\mathbf{E}}_m]_{q,k}$ is the element of $\tilde{\mathbf{E}}_m$ at its q -th row and k -th column. Now, using (28) and (55) we get

$$\begin{aligned} \mu(\tilde{\mathbf{E}}_1) &= \max_{\substack{1 \leq k, p \leq N_1 \\ k \neq p}} \frac{1}{M} |[\tilde{\mathbf{E}}_1]_k^* [\tilde{\mathbf{E}}_1]_p| \\ &= \frac{1}{M} |[\tilde{\mathbf{E}}_1]_1^* [\tilde{\mathbf{E}}_1]_2| \\ &= \frac{1}{M} \left| \sum_{q=0}^{M-1} \exp(-i2\pi q/N) \right| = \mathcal{S}(1). \end{aligned} \quad (56)$$

Furthermore, for any $\ell \neq m$ using (53) we get

$$\hat{\mu}(\tilde{\mathbf{E}}_m, \tilde{\mathbf{E}}_\ell) = \max_{1 \leq k, p \leq N_1} \frac{1}{M} |[\tilde{\mathbf{E}}_m]_k^* [\tilde{\mathbf{E}}_\ell]_p|. \quad (57)$$

Now using the expression of $[\tilde{\mathbf{E}}_m]_{q,k}$ in (55), for any $k, p \in \{1, 2, \dots, N_1\}$ with $\ell \neq m$, we have

$$\begin{aligned} &\frac{1}{M} |[\tilde{\mathbf{E}}_m]_k^* [\tilde{\mathbf{E}}_\ell]_p| \\ &= \frac{1}{M} \left| \sum_{q=0}^{M-1} \exp\left(\frac{-i2\pi q}{N} \left(\frac{n_{cs} \tilde{u}N}{M}(\ell - m) + (p - k)\right)\right) \right| \\ &= \mathcal{S}\left(\frac{n_{cs} \tilde{u}N}{M}(\ell - m) + (p - k)\right) \\ &= \mathcal{S}\left(\left(\frac{n_{cs} \tilde{u}N}{M}(\ell - m) + (p - k)\right) \bmod N\right) \end{aligned} \quad (58)$$

where in (58) we use the property (51). Denote

$$\xi(m, \ell, p, k) = \left(\frac{n_{cs} \tilde{u}N}{M}(\ell - m) + (p - k)\right) \bmod N.$$

We see that

$$\xi(m, \ell, p, k) = N - \xi(\ell, m, k, p).$$

Hence, using (50) we can express (58) as

$$\frac{1}{M} |[\tilde{\mathbf{E}}_m]_k^* [\tilde{\mathbf{E}}_\ell]_p| = \mathcal{S}(\min\{\xi(m, \ell, p, k), \xi(\ell, m, k, p)\}). \quad (59)$$

Note that for any values of m, ℓ, p and k we have $\min\{\xi(m, \ell, p, k), \xi(\ell, m, k, p)\} \in [0, N/2]$. Recall that $\mathcal{S}(r)$ is a monotonically decreasing function for $0 \leq r \leq 1$. Thus, whenever $\min\{\xi(m, \ell, p, k), \xi(\ell, m, k, p)\} \leq 1$, we have

$$\begin{aligned} &\mathcal{S}(\min\{\xi(m, \ell, p, k), \xi(\ell, m, k, p)\}) \\ &= \mathcal{S}(\min\{1, \xi(m, \ell, p, k), \xi(\ell, m, k, p)\}) \end{aligned} \quad (60)$$

On the other hand, whenever $\min\{\xi(m, \ell, p, k), \xi(\ell, m, k, p)\} > 1$, the property of $\mathcal{S}(r)$ in (52) implies that

$$\begin{aligned} &\mathcal{S}(\min\{\xi(m, \ell, p, k), \xi(\ell, m, k, p)\}) \\ &< \mathcal{S}(\min\{1, \xi(m, \ell, p, k), \xi(\ell, m, k, p)\}) \end{aligned} \quad (61)$$

Now combining (60) and (61), for any value of $\min\{\xi(m, \ell, p, k), \xi(\ell, m, k, p)\} \in [0, N/2]$ we can express (59) as

$$\frac{1}{M} |[\tilde{\mathbf{E}}_m]_k^* [\tilde{\mathbf{E}}_\ell]_p| \leq \mathcal{S}(\min\{1, \xi(m, \ell, p, k), \xi(\ell, m, k, p)\}). \quad (62)$$

Consequently using (57), for any $\ell \neq m$ we have

$$\begin{aligned} &\hat{\mu}(\tilde{\mathbf{E}}_m, \tilde{\mathbf{E}}_\ell) \\ &\leq \mathcal{S}\left(\min\left\{1, \min_{1 \leq k, p \leq N_1} \{\xi(m, \ell, p, k), \xi(\ell, m, k, p)\}\right\}\right) \end{aligned} \quad (63)$$

where the equality holds only if $\min_{k,p} \{\xi(m, \ell, p, k), \xi(\ell, m, k, p)\} \leq 1$. As a result, for any $\ell, m \in \{1, 2, \dots, G\}$

$$\max_{\ell \neq m} \hat{\mu}(\tilde{\mathbf{E}}_\ell, \tilde{\mathbf{E}}_m) \leq \mathcal{S}(\min\{1, \zeta(\tilde{u})\}) \quad (64)$$

likewise, the equality holds only if $\zeta(\tilde{u}) \leq 1$. Now combining (56) and (64) with (54), we obtain (29). ■

APPENDIX B PROOF OF THE RELATION IN (52)

By construction, $\mathcal{S}(r)$ obeys the properties of Fejér kernel [33]. The maximum of $\mathcal{S}(r)$ occurs at $r = 0$. The zeros of $\mathcal{S}(r)$ are located at the non-zero multiples of N/M . Hence, there are $(M-1)$ number of zeros of $\mathcal{S}(r)$ on $r \in [0, N-1]$. There exists only one local maximum point between every two consecutive zeros. Consequently, $\mathcal{S}(r)$ will have $(M-2)$ number of local maxima on $r \in [0, N-1]$.

Suppose that $\pi\sqrt{2} \leq M \leq N/2$. For $r \in [0, N/M]$, the only zero of $\mathcal{S}(r)$ occurs at $r = N/M$ and the maximum point is at $r = 0$. Hence, $\mathcal{S}(r)$ is a monotonically decreasing function for $0 \leq r \leq N/M$. Here, $N/M \geq 2$. Hence

$$\arg \max_{r \in [1, N/M]} \mathcal{S}(r) = 1.$$

Since $\mathcal{S}(N-r) = \mathcal{S}(r)$, we conclude that

$$\arg \max_{r \in [1, N/M] \cup [N-N/M, N-1]} \mathcal{S}(r) = 1.$$

We emphasize that, in above, N is not included in the domain over which the maximum value is sought. Let r_n is the unique local maximum point of $\mathcal{S}(r)$ located in the interval $r_n \in (nN/M, (n+1)N/M)$. It is well known that $\mathcal{S}(r_1) \geq \mathcal{S}(r_n); n \in \{1, 2, \dots, M-2\}$ [33]. As a result, for $r \in (N/M, N-N/M)$ the maximum value of $\mathcal{S}(r)$ is $\mathcal{S}(r_1)$. Hence, to prove the relation (52), it is sufficient to show that $\frac{\mathcal{S}(1)}{\mathcal{S}(r_1)} > 1$ i.e.,

$$\frac{|\text{sinc}(M/N)| |\text{sinc}(r_1/N)|}{|\text{sinc}(r_1M/N)| |\text{sinc}(1/N)|} > 1. \quad (65)$$

Note that $r_1 \in (N/M, 2N/M)$. By differentiating $\text{sinc}(rM/N)$ with respect to r and equating to zero, it can be verified that the local maximum point of $|\text{sinc}(rM/N)|$ for $r \in (N/M, 2N/M)$ occurs at [34]

$$\tilde{r} = \left[3/2\pi - \frac{2}{3\pi}\right] \frac{N}{\pi M} = 1.4325 \frac{N}{M}.$$

Hence,

$$|\text{sinc}(r_1M/N)| \leq |\text{sinc}(\tilde{r}M/N)| = 0.6824/\pi. \quad (66)$$

The power series expansion of $\text{sinc}(x)$ is [35]

$$\text{sinc}(x) = \sum_{n=0}^{\infty} (-1)^n \frac{(\pi x)^{2n}}{(2n+1)!}. \quad (67)$$

Now using (67), we have

$$\text{sinc}(r_1/N) = 1 - \frac{(\pi r_1/N)^2}{3!} + \sum_{n=2}^{\infty} t_n \quad (68)$$

where, $t_n = (-1)^n \frac{(\pi r_1/N)^{2n}}{(2n+1)!}$. In particular, if $|\pi r_1/N| < \sqrt{48}$ then for all non-zero positive integer k i.e., for $k \in \mathbb{Z}_{>0}$ we have

$$\begin{aligned} t_{2k} + t_{2k+1} &= \frac{(\pi r_1/N)^{4k}}{(4k+1)!} - \frac{(\pi r_1/N)^{4k+2}}{(4k+3)!} \\ &= \frac{(\pi r_1/N)^{4k}}{(4k+1)!} \left\{ 1 - \frac{(\pi r_1/N)^2}{(4k+2)(4k+3)} \right\} \\ &\geq \frac{(\pi r_1/N)^{4k}}{(4k+1)!} \left\{ 1 - \frac{48}{6 \cdot 8} \right\} = 0 \end{aligned} \quad (69)$$

where in the last inequality we set $k = 1$. Hence, $\sum_{n=2}^{\infty} t_n = \sum_{k=1}^{\infty} (t_{2k} + t_{2k+1}) \geq 0$. Since $r_1 \in (N/M, 2N/M)$ and $M \geq \pi\sqrt{2}$, hence $\pi r_1/N < 2\pi/M \leq \sqrt{2}$. Now from (68), we get

$$|\text{sinc}(r_1/N)| > 1 - \frac{(\pi r_1/N)^2}{6} > 2/3. \quad (70)$$

Since $N/M \geq 2$, hence $\pi M/N \leq \pi/2$. Then using a similar procedure of (68), we get

$$|\text{sinc}(M/N)| > 1 - \frac{(\pi M)^2}{6N^2} \geq 1 - \frac{\pi^2}{24}. \quad (71)$$

Now combining (66), (70), (71) and the fact $|\text{sinc}(1/N)| \leq 1$, we obtain the bound in (65).

APPENDIX C PROOF OF PROPOSITION-2

Using the expression of $[\tilde{\mathbf{E}}_\ell]_{n,k}$ in (55), we see that for any $k, p \in \{1, 2, \dots, N_1\}$ with $\ell \in \mathcal{J}_{u_1}$; $m \in \mathcal{J}_{u_2}$ and $u_1 \neq u_2$, we have

$$\begin{aligned} &\frac{1}{M} |[\tilde{\mathbf{E}}_\ell]_k^* [\tilde{\mathbf{E}}_m]_p| \\ &= \frac{1}{M} \left| \sum_{n=0}^{M-1} \exp \left(\frac{-i\pi}{M} [(u_2 - u_1)(n^2 + n) \right. \right. \\ &\quad \left. \left. + 2n \left\{ n_{cs} (u_2(m-1) - u_1(\ell-1)) + (p-k) \frac{M}{N} \right\}] \right) \right| \\ &= \frac{1}{M} \left| \sum_{n=0}^{M-1} \exp \left(-i \frac{\pi}{M} (u_2 - u_1) \left[\{n + \vartheta(u_1, u_2, \ell, m, p, k)\}^2 \right. \right. \right. \\ &\quad \left. \left. - \vartheta(u_1, u_2, \ell, m, p, k)^2 \right] \right) \right| \\ &= \frac{1}{M} \left| \exp \left(i \frac{\pi}{M} (u_2 - u_1) \vartheta(u_1, u_2, \ell, m, p, k)^2 \right) \right. \\ &\quad \left. \sum_{n=0}^{M-1} \exp \left(-i \frac{\pi}{M} (u_2 - u_1) \left[(n + \vartheta(u_1, u_2, \ell, m, p, k))^2 \right] \right) \right| \end{aligned}$$

which implies (43).

REFERENCES

- [1] "3rd Generation Partnership Project; technical specification group radio access network; evolved universal terrestrial radio access (E-UTRA); physical channels and modulation (release 10)."
- [2] "IEEE standard for local and metropolitan area networks part 16: Air interface for broadband wireless access systems," *IEEE Std 802.16-2009 (Revision of IEEE Std 802.16-2004)*, pp. 1–2080, 2009.
- [3] L. Sanguinetti and M. Morelli, "An initial ranging scheme for the IEEE 802.16 OFDMA uplink," *Wireless Communications, IEEE Transactions on*, vol. 11, no. 9, pp. 3204–3215, 2012.
- [4] M. Ruan, M. Reed, and Z. Shi, "Successive multiuser detection and interference cancellation for contention based OFDMA ranging channel," *Wireless Communications, IEEE Transactions on*, vol. 9, no. 2, pp. 481–487, 2010.
- [5] C.-L. Lin and S.-L. Su, "A robust ranging detection with MAI cancellation for OFDMA systems," in *Advanced Communication Technology (ICACT), 2011 13th International Conference on*, 2011, pp. 937–941.
- [6] L. Sanguinetti, M. Morelli, and L. Marchetti, "A random access algorithm for LTE systems," *Transactions on Emerging Telecommunications Technologies*, vol. 24, no. 1, pp. 49–58, 2013. [Online]. Available: <http://dx.doi.org/10.1002/ett.2575>
- [7] D. Chu, "Polyphase codes with good periodic correlation properties (corresp.)," *Information Theory, IEEE Transactions on*, vol. 18, no. 4, pp. 531–532, Jul 1972.
- [8] R. Frank and S. Zadoff, "Phase shift pulse codes with good periodic correlation properties (corresp.)," *Information Theory, IRE Transactions on*, vol. 8, no. 6, pp. 381–382, October 1962.
- [9] M. Gul, X. Ma, and S. Lee, "Timing and frequency synchronization for OFDM downlink transmissions using Zadoff-Chu sequences," *Wireless Communications, IEEE Transactions on*, vol. 14, no. 3, pp. 1716–1729, March 2015.
- [10] S. Sesia, I. Toufik, and M. Baker, *LTE - the UMTS long term evolution : from theory to practice*. Chichester: Wiley, 2009. [Online]. Available: <http://opac.inria.fr/record=b1130916>
- [11] M. Hua, M. Wang, W. Yang, X. You, F. Shu, J. Wang, W. Sheng, and Q. Chen, "Analysis of the frequency offset effect on random access signals," *Communications, IEEE Transactions on*, vol. 61, no. 11, pp. 4728–4740, November 2013.
- [12] C.-L. Wang, H.-C. Wang, and Y.-H. Chen, "A synchronization scheme based on interleaved partial Zadoff-Chu sequences for cooperative MIMO systems," in *Vehicular Technology Conference (VTC Fall), 2013 IEEE 78th*, Sept 2013, pp. 1–5.
- [13] J.-C. Guey, "The design and detection of signature sequences in time-frequency selective channel," in *Personal, Indoor and Mobile Radio Communications, 2008. PIMRC 2008. IEEE 19th International Symposium on*, Sept 2008, pp. 1–5.
- [14] G. Wunder, P. Jung, and C. Wang, "Compressive random access for post-LTE systems," in *Communications Workshops (ICC), 2014 IEEE International Conference on*, June 2014, pp. 539–544.
- [15] E. J. Candés and M. B. Wakin, "An introduction to compressive sampling," *IEEE Signal Processing Magazine*, vol. 25, pp. 21–30, mar 2008.
- [16] E. J. Candés, J. Romberg, and T. Tao, "Robust uncertainty principles: exact signal reconstruction from highly incomplete frequency information," *IEEE Transactions on Information Theory*, vol. 52, pp. 489–509, Feb. 2006.
- [17] Y. Zhou, Z. Zhang, and X. Zhou, "OFDMA initial ranging for IEEE 802.16e based on time-domain and frequency-domain approaches," in *Communication Technology, 2006. ICCT '06. International Conference on*, 2006, pp. 1–5.
- [18] B. Popovic, "Generalized chirp-like polyphase sequences with optimum correlation properties," *Information Theory, IEEE Transactions on*, vol. 38, no. 4, pp. 1406–1409, Jul 1992.
- [19] X. Fu, Y. Li, and H. Minn, "A new ranging method for OFDMA systems," *Wireless Communications, IEEE Transactions on*, vol. 6, no. 2, pp. 659–669, 2007.
- [20] S. Beyme and C. Leung, "Efficient computation of dft of zadoff-chu sequences," *Electronics Letters*, vol. 45, no. 9, pp. 461–463, April 2009.
- [21] B. Popovic, "Efficient dft of zadoff-chu sequences," *Electronics Letters*, vol. 46, no. 7, pp. 502–503, April 2010.
- [22] E. Dahlman, S. Parkvall, and J. Skold, *4G: LTE/LTE-Advanced for Mobile Broadband*, 1st ed. Academic Press, 2011.
- [23] R. Tibshirani, "Regression shrinkage and selection via the Lasso," *Journal of the Royal Statistical Society, Series B*, vol. 58, pp. 267–288, 1994.

- [24] J. Tropp, “Just relax: convex programming methods for identifying sparse signals in noise,” *Information Theory, IEEE Transactions on*, vol. 52, no. 3, pp. 1030–1051, March 2006.
- [25] E. J. Candès and T. Tao, “Decoding by linear programming,” *IEEE Transactions on Information Theory*, vol. 51, pp. 4203–4215, Dec. 2005.
- [26] E. J. Candès, J. Romberg, and T. Tao, “Stable signal recovery from incomplete and inaccurate measurements,” *Communications on Pure and Applied Mathematics*, vol. 59, pp. 1207 – 1223, Mar. 2006.
- [27] Z. Ben-Haim, Y. Eldar, and M. Elad, “Coherence-based performance guarantees for estimating a sparse vector under random noise,” *Signal Processing, IEEE Transactions on*, vol. 58, no. 10, pp. 5030–5043, Oct 2010.
- [28] A. Tillmann and M. Pfetsch, “The computational complexity of the restricted isometry property, the nullspace property, and related concepts in compressed sensing,” *Information Theory, IEEE Transactions on*, vol. 60, no. 2, pp. 1248–1259, Feb 2014.
- [29] D. Donoho, M. Elad, and V. Temlyakov, “Stable recovery of sparse overcomplete representations in the presence of noise,” *Information Theory, IEEE Transactions on*, vol. 52, no. 1, pp. 6–18, Jan 2006.
- [30] P. Alfeld. (1998) A proof of the reverse triangle inequality. [Online]. Available: <http://www.math.utah.edu/~pa/math/equations/proof.html>
- [31] D. Sarwate, “Bounds on crosscorrelation and autocorrelation of sequences (corresp.),” *Information Theory, IEEE Transactions on*, vol. 25, no. 6, pp. 720–724, November 1979.
- [32] Y. Xie, Y. Eldar, and A. Goldsmith, “Reduced-dimension multiuser detection,” *Information Theory, IEEE Transactions on*, vol. 59, no. 6, pp. 3858–3874, June 2013.
- [33] A. Zygmund, *Trigonometric Series (Vol. 2)*. Cambridge University Press, 2002.
- [34] A. Wiggins. (2007) The minimum of the Dirichlet kernel. [Online]. Available: <http://www-personal.umd.umich.edu/~adwiggins/>
- [35] L. Råde and B. Westergren, *Mathematics Handbook for Science and Engineering*. Secaucus, NJ, USA: Birkhauser Boston, Inc., 1995.